BIODETECTION OF ENVIRONMENTAL MARINE CONTAMINANTS USING REGENERATED BIOSENSORS: THE IRGAROL CASE STUDY

M. López de Miguel[a*], J.Pablo Salvador[b,c], F. Palacio[a], F. Arreza[a], A. Diéguez[a] and J.D. Prades[a*]

[a] Departament d'Enginyeria Electrònica i Biomèdica, Universitat de Barcelona, C/ Martí i Franquès 1, E-08028 Barcelona, Spain
[b] Nanobiotechnology for diagnostics (Nb4D), Department of Chemical and Biomolecular Nanotechnology, Institute for Advanced Chemistry of Catalonia (IQAC) of the Spanish Council for Scientific Research (CSIC), Barcelona, Spain
[c] CIBER de Bioingeniería, Biomateriales y Nanomedicina (CIBER-BBN), Jordi Girona 18-26, E-08034 Barcelona, Spain

[*]Corresponding authors e-mail: manel.lopez@ub.edu and dprades@ub.edu

Abstract:

A low-cost and low-powered electro-mechanical device was designed and tested to perform a continuous monitoring tracking of sea contaminants. In particular, we focus our work on the biodetection of Irgarol, a specific seawater contaminant, selected as a proof-of-concept for the measurement system. The device based its measurement on a continuous analyte flow mode over the sensor cavity, followed by a sensor cleaning and regeneration process, which will prepare the sensor for the next measurement. All the system was designed to prioritize accuracy and repeatability

Keywords: Amperometry, marine contaminants, regenerated biosensors.

1. INTRODUCTION

Marine regions account for over 40% of Europe's gross domestic product (GDP) [1], being between 3 and 5% of the latter generated directly from marine-based services and industries [2, 3]. In this context, chemical contamination of estuarine and coastal areas implies terrible consequences for the environment and through the food chain for public health. Current analytical techniques for the detection of environmental pollutants are considered the best way to validate and confirm screening techniques [4]. However, they present a major problem: they require preconcentration and clean-up strategies, qualified personnel and complex instrumentation that results in a high cost/analysis ratio. To reach enough exhaustive measurements, it is necessary to be able to carry out the measurements quickly and simply, process the data, compare, and provide an accurate result from techniques based on data processing, and at the lowest possible cost.

Current analytical techniques for the detection of environmental pollutants are based on chromatographic techniques coupled to mass spectrometric detectors in centralized laboratories [5]. These well-known methods can measure extremely low concentrations of analytes solved in liquids, providing high detectability, specificity,

and multianalyte analysis, and are considered as the golden standard methodology for the validation and confirmatory method of screening techniques. However, they require preconcentration and clean-up strategies, qualified personnel, and complex instrumentation that results in a high cost/analysis ratio. In order to reach enough detectability to monitor on-time environmental pollutants, it is required to develop rapid, simple, and low-cost devices.

Immunosensors make use of the specific binding between an antibody and antigen coupled to a physical transducer that converts the biorecognition process into a measurable signal [6]. The antigen-antibody interaction is the basis of a wide variety of immunochemical methods selective and sensitive enough to detect organic pollutants. Immunoassays have been widely used in environmental applications [7] as a high throughput method allowing the simultaneous analysis of several samples. These can be adapted to rapid detection formats such as dip-sticks or presented in combination with other transducer elements [8]. The development of an autonomous and automatic device based on amperometric was the transduction principle chosen in this work.

2. DESCRIPTION OF THE WORK

The measurement system was designed to measure during a long period of time, two different contaminants simultaneously and in a continuous way (Figure 1). Once the measurement is done, the sensor must be cleaned, adding a NaOH 0.3M solution, regenerated, and prepared to be reused [9]. In this sense, the tanks presented in Figure 1 are necessary to perform the sensor preparation, regeneration, and recycling. Figure 1a shows the block diagram of the device and Figure 1b presents the final system prepared for testing in lab conditions. Specifically, the demonstration was performed using immunoreagents for the

determination of a well-known photosynthesis-inhibiting herbicide: Irgarol 1051® [9], a triazine herbicide that is being used as antifouling paint on watercraft hulls to prevent algae growth. This contaminant is an algaecide used as an antifoulant paints to control fouling organisms on the hulls of recreational and commercial watercraft. Irgarol 1051®, henceforth Irgarol, act over aquatic ecosystems, generating an important ecological risk in marinas, estuaries, and coastal waters, being much more toxic to marine plants than animals. In a detailed study of the effect of Irgarol in coastal water microcosms, Björn et al. [13], have shown how Irgarol inhibits the photosynthetic activity at 3.2nM in short-term (hours) test. Moreover, for long-term (weeks) exposure, the effect of the contaminant is significant, even for lower concentrations (1nM).

The Electro-Microfluidic System (EMS) is composed by two important blocks, Paragraph 2.1 defines the Immunosensor protocol, hardware, tubing, peristaltic micro-pumps and micro-valves, the different liquid repositories to store the different elements needed for the detection of Irgarol, cleaning and sensor regeneration, and finally explains the protocol that makes everything work. Paragraph 2.2 enters in depth in the development of the electronic control system and the software necessary to process the acquired data

2.1 Immunosensor Protocol and Microfluidic System

2.1.a Immunosensor Protocol

Immunoreagent pair 4e-BSA/As87 (4e-BSA: Bovine serum albumin coupled to a Hapten 4e; Hapten: molecule that mimic the target analyte to be coupled to a carrier protein to induce immune response; As87: antiserum specific for Irgarol) were selected for the detection of our target contaminant. There is an extense literature that explains how well this couple of elements works in such detection [6, 11, 14]. Irgarol has been studied widely by the scientific community using different techniques such as ELISA [11], fluorescent microarray [11], optical [12] and electrochemical immunosensors [9, 10].

Due to the extremely low concentration of Irgarol in seawater, the measurement of this contaminant requires a preconcentration process. To do this, the device implements a disposable Solid Phase Extraction (SPE) cartridge. When the preconcentration stage finish, the resulting elute is sent to the mixing tank (see figure 1a), where it is mixed with As87. The combined product is sent to the biosensor µchamber, where the coating antigen 4e-BSA was previously immobilized on the surface of the biosensor.

The As87 can react with both Irgarol and 4e-BSA. If there is an excess of Irgarol in the analyte, all the As87 will react with Irgarol in the mixing tank. As As87 was neutralized with Irgarol, it cannot combine with 4e-BSA meaning a low or nil current signal. On the contrary, when the concentration of Irgarol is very low or nil, the antigen-antibody reaction that takes place is the 4e-BSA/As87, which generates a maximum in the current signal. To summarize, the low current signal means a high Irgarol concentration, and on the contrary, the high current signal will mean a low Irgarol concentration.

2.1.b The Microfluidic system

To perform the measurement repetitively and be able to measure over a long period of time, a number of tanked reagents linked to the microfluidic system are required. This is depicted in Figure 1a, where a scheme of the mixture and measurement flow pathways, including the required peristaltic micropumps and microvalves necessary to perform the process, is shown. Basically, it requires a tank containing Phosphate Buffered Saline buffer with Tween® 20 (PBST) to perform both the washes between stages and the conditioning of the biosensor chambers. The Antibody buffer (ABB) tank supplies the specific antibodies for the recognition of the target analyte. The sample is pushed and addressed to the Dilution tank (DT) by a peristaltic micropump, where it is combined with the antibody for the analyte-antibody preincubation. After a period of 25 min, the content is flooded to the biosensor chambers. The device requires the inclusion of the anti-IgG-HRP conjugate, used as a catalyzer of the 4e-BSA/As87 reaction, the detection solution, and the regeneration solution, which are stored in the aHRP, detection solution (DS) and regeneration solution (RS) tanks respectively. A complete description of the measurement, cleaning and regeneration process can be found at [9]. With these characteristics, the limit of detection reached was 0.15±0.09 nM (0.038±0.022 $\mu g \cdot L^{-1}$) measured directly in seawater. Finally, a technical issue is important to remark, according to the peristaltic pump used, a minimum flow rate was used and set at 0.027 ml/s in all the steps, to favor the analyte-antibody interaction. Figure 1b shows a picture of the final device.

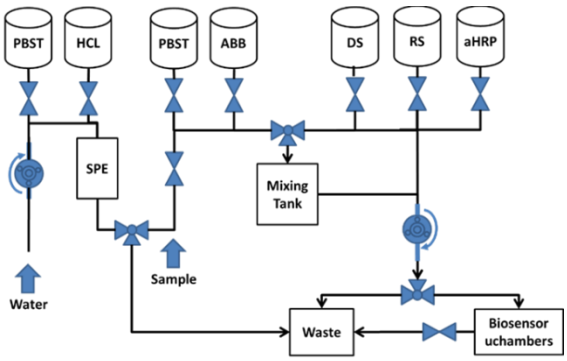

(a)

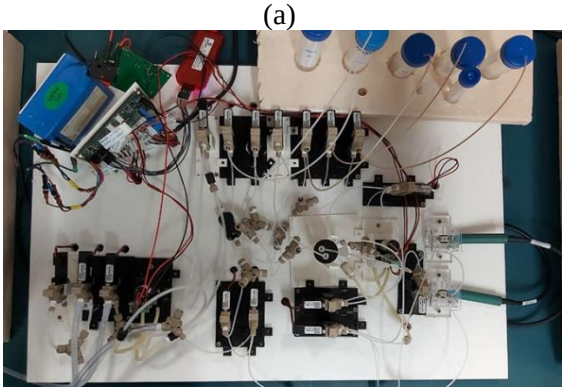

(b)

Figure 1. (a) Schematic of the microfluidic network controlled by peristaltic micropumps and microvalves through which the reagents flow to the biosensor µchambers and eventually to waste. Tanks contain PBST, Detection solution (DS), Regeneration Solution (RS) and the anti-IgG-HRP conjugate solution (aHRP). (b) Image of the system. The two manifolds are at upper border of the system. In the middle, the SPE, the different micropumps and microvalves can be seen. In the botton right the sensor µchambers.

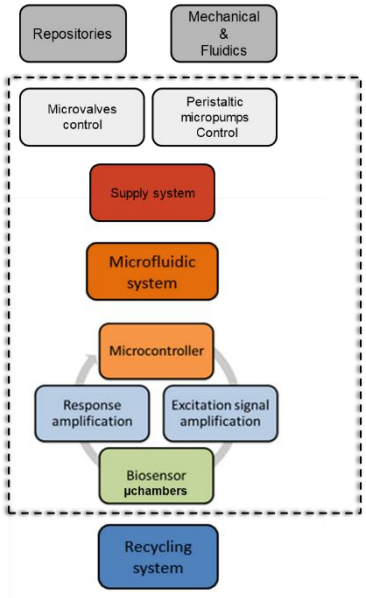

Figure 2. Block diagram of the electronic system

2.2 Electronic System and Data Processing

The electronic system is the responsible of: (i) controlling the functionality of the different µvalves and peristaltic µpumps; (ii) implementing the algorithm that will move the chemical products to the different chambers in the proper way; (iii) preparing the sensing chamber to perform the measurement; (iv) filtering and processing the data; finally (v) managing the cleaning process and activate the regeneration of the sensors to be able to carry out new measurements. The acquisition is done by the analog-to digital-port integrated in the microcontroller. Data are pre-processed and transmitted to the central unit (a PC or laptop) where the final data process is done. Figure 2 shows a block diagram presenting the most important characteristics of the electronic system. The digital part is based on a 32-bit PIC32MX795F512L (Microchip corp.) microcontroller, in which the management firmware necessary to control the measurement process has been loaded. The analog part is based on a miniaturized potentiostat for measuring amperometric biosensors. The activation of the microvalves was done using eight of the microcontroller's digital outputs, which excited the gate of eight RTR020N05 NMOSFET transistors (RHOM), one for every microvalve, allowing the fluids pass to the different sensor µchambers. The different sensors were excited with -0.1V between the reference and the working electrodes using the potentiostat based on an OPA2182 (Texas Instruments) operational amplifier.

The -0.1V corresponds to the best signal to be applied to the immobilizer TMB, used as an electron transfer mediator in our amperometric biosensor. Pulse width modulation (PWM) was used to generate this -0.1V. The signal of the PWM was directly connected to a Sallen-Key 1Hz low-pass filter, based on an OPA2182, to obtain a clean-of-noise reference. The response of the sensor signals was acquired by eight very high input impedance LPC662A OPAMP, configured as trans-impedance operational amplifier (TIA). The feedback loops were used for measuring three-lead electrochemical biosensors. The output of this TIA was filtered and directly connected to the microcontroller's Analog Digital Converter (ADC) inputs. To perform the in-situ signal processing, we took advantage of its 80 MHz, 1.56 DMIPS, and Mk4 core with five stage pipeline Harvard architecture.

3. Measurement System process, calibration and validation

3.1 Determination of the calibration curve

The determination of a calibration curve based on well-known concentration results is necessary to subsequently determine the concentration of Irgarol in real conditions. To perform this analysis, five samples with a well-known Irgarol concentration were measured. These five samples had concentrations of 10^{-1}, 5, 20, 200 and 10^3 nM. Figure 3.a represents the evolution of the sensor signal over time. The time needed to stabilize the antigen-antibody reaction is estimated at around 75 seconds for all the samples. Figure 3.b summarizes this signal-plateau-level vs. the Irgarol concentration. The obtained values are fitted to a Four Parameter Logistic (4PL) curve, a common regression model used to analyze bioassays.

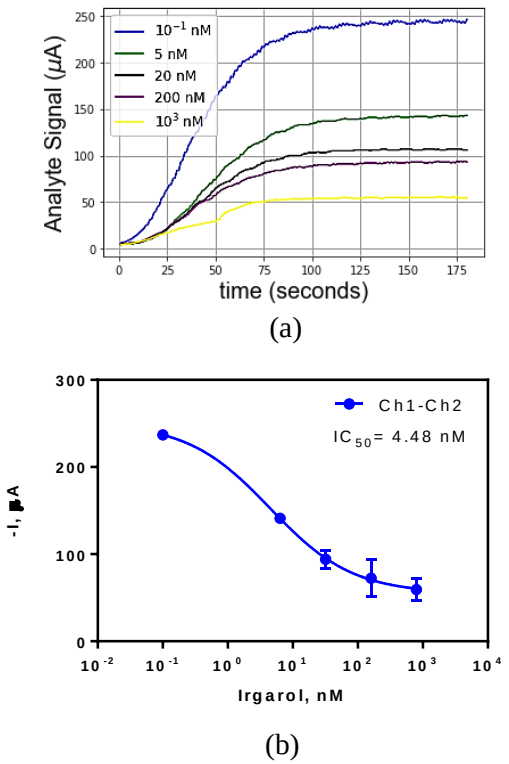

Figure 3. (a) Evolution of the measured signal over time for different Irgarol concentration. (b) Calibration curve for Irgarol determination as a function of the current. The data represented is the average of two channels tested.

4PL curves (Equation 1) are very useful for characterizing bioassays because there is only linear across a specific range of concentration magnitudes. Beyond this linear range, the responses quickly plateau and approach the minimum and maximum. The name of the curve refers to four parameters: (i) Minimum or point of smallest response, D in our case. It can be a baseline, control, or response for nil concentration. (ii) Maximum or greatest response. A in our case. (iii) Inflection point, C, corresponding with the dose at which the curvature of the response line changes; where the rate of change switches signs; often referred to as the IC50 or EC50. (iv) Hill coefficient, B. The slope of the curve at the inflection point [15].

$$y = \frac{(A-D)}{(1+(x/C)^B} + D \qquad (1)$$

```python
from scipy.optimize import curve_fit
import numpy as np
from sklearn.metrics import r2_score
from sklearn.metrics import mean_squared_error as mse
from sklearn.metrics import r2_score

def fourPL(x, A, B, C, D):
    y= ((A-D)/(1.0+((x/C)**(B))) + D)
    if y is np.nan or y is np.inf:
        print(y, x)
        sys.exit(0)
    return y

def fitted_sigmoidal(x,A,B,C,D):
    return A/(B+C*np.exp(D*x))

params, params_covariance = curve_fit(fourPL, ch_concentration, ch_mean, maxfev = 100000)

xs = np.linspace(x_min, x_max, 10000)
print("fourPL adjustemt parameters: ", params)
y_predict =((params[0]-params[3])/(1.0+((ch_concentration/[params[2]]))**(params[1])))+params[3])

print("Mean Square Error: %.2f" %mse(ch_mean, y_predict))
print("R^2 square: %.2f" %r2_score(ch_mean, y_predict))
y =fourPL(xs, *params2)
plt.semilogx(xs, y, color="blue")
plt.semilogx(ch_concentration, ch_mean, "o")
plt.yticks([0,100,200,300])
plt.xlim([1E-2, 1E4])
plt.ylim([0, 300])
plt.xlabel('Irgarol, nM', fontname="Arial", fontsize="20")
plt.ylabel('-I, $\mu A$', fontname="Arial", fontsize="20")
```

Figure 4. Python script that calculates the four parameters of the 4PL curve. Lines 23 and 24 permit to calculate the performance of the adjustment. From line 25 and bellow the code to obtain figure 2b.

Figure 4 shows the code designed to adjust the mean parameters to the 4PL curve. The programming language used to perform this analysis was Python. We also included powerful libraries to accelerate the software design and decrease the processing time. In particular, we use the curve fit function, included in the optimization library of the SciPy API. This method applies non-linear least squares to fit the data to a proposed theoretical function and extract the optimal parameters that better adjust the function with the experimental data. We also import from the package sklearn the library metrics, which include the r2_score and the mean square error (MSE). R^2 indicates the proportion of data points which lie within the function created by the curve fit method. A higher value of R^2 indicates a better adjustment. $R^2 \leq 1$. This library also includes the MSE, which measures the amount of error in statistical models. It assesses the average squared difference between the observed and the predicted values. No difference between observable and predictable points provides a MSE equal to zero. Table 1 presents the response of the simulation, including r2 score and MSE.

Table 1. Four logistic equation parameters.

Bottom	Top	HillScope	IC50	R2 scr	MSE
54.87	250.4	-0.6837	4.48	0.99	1.38

Being r2 score and MSE the regression score function and the function that computes a risk metric corresponding to the expected value of the squared logarithmic error or loss respectively.

3.2 Measurement validation

Four new measurements were done to validate the system. Now, Irgarol concentrations where ranged at 0.3, 1.6, 10, and 50 nM. Two different sets of samples were performed for these concentration ranges to increase the number of measurements. The reason for choosing this concentration range is because of they belong to the linear evolution of the 4PL curve. Figure 5 shows their evolution compared with the 4PL calibration curve. Figure 5 shows both the measurement of the first and the second set of samples as green triangles, and orange squares respectively, the main points used to generate the calibration curve as blue circles and the calibration curve itself as the blue line.

Table 2 presents the measured response of these points, including the evaluation of the r2 score and MSE for both measurements.

Table 2. Signal response of the validation samples

	0.3nM	1.6nM	10nM	50nM	R2	MSE
Set 1	225.2	129.8	120.0	80.1	0.72	801.5
Set 2	230.1	200.2	138.1	100	0.95	141.8

The low value of r2 score and high number in MSE for Set 1 is clearly related to the sample synthesized at 1.6 nM. It is perfectly observable in Figure 5, where there exists a big difference between this point and the one that belongs to set 2 and the calibration curve and can be considered as a wrong value. Without this value, Set 1 would have an r2 score of 0.92. Set 2 has a very nice value of r2 score, 0.95, matching almost perfectly with the calibration curve.

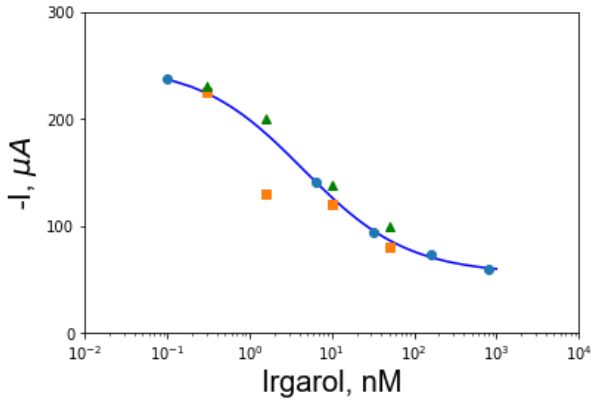

Figure 5. Representation of two sets of samples, green triangles and orange squares synthesized in the linear range of the 4PL curve. Blue circles correspond to the mean values of the validation curve (blue line).

4. SUMMARY

This work reports on the design of a low-cost and portable device for seawater pollutants in continuous monitoring. The sensor used can be regenerated after the measurement process and prepared to be used again. It was tested by measuring Irgarol 1051. We choose this contaminant due to the deep knowledge that we have about it and presented in different publications [7-10]. The work here presented was performed by measuring in lab conditions the contaminant at different concentrations and different days, collecting the necessary data to perform a calibration curve based on a four-parameter logistic regression (4PL curve). To do this, an embedded acquisition system was designed, developed, and tested. The acquisition system was based on a MIPS 32 microcontroller architecture (Microchip ©), which permits to manage the different chemical repositories, microvalves, micropumps, and microchambers necessary to deliver the chemicals to the different microchambers were the reactions take place, to prepare the final analyte for the final antigen-antibody measurement, necessary to determine the Irgarol concentration, process the acquired data and regenerating the sensor to perform new measurements.

The calibration curve was tested with two different sets of samples synthesized at the same concentrations, obtaining an r2 score after a proper analysis of the results above 90%.

All the measurements were done using the same sensors, which were cleaned and regenerated once the measurements were concluded.

5. REFERENCES

[1] J. Baten, A History of the Global Economy: 1500 to the Present, Cambridge: Cambridge University Press; 2016.

[2] J. Bostock, A. Lane, C. Hough, K. Yamamoto, Aquaculture International, 24(2016) 699-733.

[3] EC, Communication from the Commission to the European Parliament, the Council, the European Economic and Social Committee and the Committee of the Regions, COM(2014) 254 final/2, (2014).

[4] M. Farré, L. Kantiani, M. Petrovic, S. Pérez, D. Barceló, Journal of Chromatography A, 1259(2012) 86-99.

[5] M. Farré, L. Kantiani, M. Petrovic, S. Pérez, D. Barceló, Achievements and future trends in the analysis of emerging organic contaminants in environmental samples by mass spectrometry and bioanalytical techniques, Journal of Chromatography A, 1259(2012) 86-99.

[6] J.P. Salvador, J. Adrian, R. Galve, D.G. Pinacho, M. Kreuzer, F. Sánchez-Baeza, et al., Chapter 2.8 in: M. Petrovic, D. Barceló (Eds.), Comprehensive Analytical Chemistry, Elsevier2007, pp. 279-334.
[7] M.-P. Marco, S. Gee, B.D. Hammock, Trends Anal Chem, 14(1995) 415-25.
[8] M.-P. Marco, S. Gee, B.D. Hammock, Trends Anal Chem, 14(1995) 341-50.
[9] J.P. Salvador, M.P. Marco, Electroanalysis, 28(2016) 1833.
[10] B. Ballesteros, D. Barceló, F. Camps, M.-P. Marco, Anal Chim Acta, 347(1997) 139-47.
[11] A. Sanchis, J.P. Salvador, K. Campbell, C.T. Elliott, W.L. Shelver, Q.X. Li, et al., Talanta, 184(2018) 499-506.
[12] B. Chocarro-Ruiz, S. Herranz, A. Fernández Gavela, J. Sanchís, M. Farré, M.P. Marco, et al. Biosensors and Bioelectronics, 117(2018) 47-52.
[13] D. Björn, H. Blanck, Marine pollution Bulletin, 32, 4(1996), 342-350.
[14] J.-Pablo Salvador, M.-Pilar Marco, G. Saviozzi, C. Laschi, F. Arreza, F. Palacio and M. López, Sensing and bio-sensing research, 37(2022), 100505
[15] https://www.aatbio.com/tools/four-parameter-logistic-4pl-curve-regression-online-calculator